distinguish between Leu-5 and Leu-17, information from NOEs between different nonlabeled residues was needed in addition to that contained in Figure 1, as is indicated in Figure 2.

On the basis of the sequence-specific assignments, Figure 1 provides direct information on the secondary polypeptide structure near several [2-^{15}N]Leu residues. Thus both Leu-Leu dipeptide segments are located in α-helices, as evidenced by the strong sequential NOEs d_{NN} throughout the polypeptide segments 49-54 and 63-66 (Figure 1A,B) and by the short distances $d_{\alpha N}$ (48, 51) and $d_{\alpha N}$ (50, 53).[1,14] Similarly, there is evidence that Leu-24 is located in a helical segment of the polypeptide chain.

In conclusion, the experiments described here illustrate that isotope labeling of a *single*, strategically selected amino acid type in a protein (Figure 2) can dramatically enhance the power of ^{1}H NMR for studies of such systems, provided that labeling is used in combination with sequential assignment procedures.[1,3,4] The latter can be greatly facilitated by the ease with which distinct resonance lines are observed in the labeled protein (Figure 1). Once sequence-specific assignments are obtained, site-directed information on the spatial polypeptide structure or on interactions with other molecules can be collected in systems which might otherwise be too complex for detailed investigations. The present experiments are part of the first phase of an investigation aimed at studies of protein-DNA interactions in the P22 c2 operator system. We plan to use protein analogues with ^{15}N labels on amino acids that are likely to be in direct contact with the DNA. The resulting NOEs can then be measured in the simplified ^{1}H NOESY spectra obtained with the ^{15}N half-filter technique, where intermolecular ^{1}H-^{1}H NOEs between ^{15}NH's and nonlabeled protons would appear as doublets along ω_2 (Figure 1B,C). Compared to the recently described X-filter technique,[15] which selects for peaks connecting protons which are *both* bound to the *same* X-spin, the half-filter experiment[12] used here can thus be combined with suitable residue-selective isotope labeling for novel investigations of structural and functional features in proteins.

Acknowledgment. Financial support was provided by the Schweizerischer Nationalfonds (Project 3.198-9.85). We thank Dr. R. Sauer for a gift of the *E. coli* strain W3110 *lac* $I^Q/_pTP$ 125 and Mrs. M. Schütz for the careful preparation of the manuscript.

(14) Wüthrich, K.; Billeter, M.; Braun, W. *J. Mol. Biol.* **1984**, *180*, 715-740.

(15) Wörgötter, E.; Wagner, G.; Wüthrich, K. *J. Am. Chem. Soc.* **1986**, *108*, 6162-6167.

Effect of Ligand on Ring Contraction of Six-Membered Nickel-Containing Cyclic Esters, $L_nNiCH_2CH_2CH_2COO$, to Their Five-Membered-Ring Isomers, $L_nNiCH(CH_3)CH_2COO$. Kinetic and Thermodynamic Control of Asymmetric Induction by Chiral Diphosphines in the Ring Contraction

Takakazu Yamamoto,* Kenji Sano, and Akio Yamamoto

Contribution from the Research Laboratory of Resources Utilization, Tokyo Institute of Technology, 4259 Nagatsuta, Midori-ku, Yokohama 227, Japan. *Received May 27, 1986*

Abstract: Ring contraction of $L_nNiCH_2CH_2CH_2COO$ (**1**) to $L_nNiCH(CH_3)CH_2COO$ (**2**) is accelerated by coordination of bulky ligands: coordination of a bulky diphosphine like 1,2-bis(diphenylphosphino)ethane (dpe) causes an extensive ring contraction to afford (dpe)$NiCH(CH_3)CH_2COO$. Use of a chiral diphosphine affords a mixture of unequal amounts of diastereomers (chiral diphosphine)-(*R*)-$NiCH(CH_3)CH_2COO$ ((*R*)-**2**) and (chiral diphosphine)-(*S*)-$NiCH(CH_3)CH_2COO$ ((*S*)-**2**). When (*S*,*S*)-chiraphos is used, (*R*)-**2** is kinetically favored, but it isomerizes to thermodynamically favored (*S*)-**2** obeying the first-order kinetics. The equilibrated reaction mixture after the isomerization contains ((*S*,*S*)-chiraphos)$NiCH(CH_3)CH_2COO$ in 54% diastereomer excess at 24 °C, and the kinetic and thermodynamic parameters for the *R* to *S* isomerization are as follows: $\Delta H^\ddagger = 93 \pm 2$ kJ/mol, $\Delta S^\ddagger = -8 \pm 6$ J/(K mol), $\Delta G^\ddagger = 95$ kJ/mol, $\Delta H° = 13 \pm 2$ kJ/mol, $\Delta S° = 54 \pm 6$ J/(K mol), and $\Delta G° = -3.0$ kJ/mol at 24 °C. Use of (*R*,*R*)-dipamp gives a result opposite to that of (*S*,*S*)-chiraphos concerning the kinetically and thermodynamically favored species. Data obtained by use of (*R*)-prophos, *trans*-cypenphos, and *trans*-renorphos are also given. The kinetic and thermodynamic control of the asymmetry can be explained by considering the effects of arrangement of two phenyl groups bonded to each phosphorus atom of the diphosphine ligands on the metallacycle entity.

Isomerization processes involving β-hydrogen elimination and reinsertion mechanism[1-7] have been considered responsible for skeletal isomerization in metal-catalyzed homogeneous catalytic reactions as well as in isolated transition-metal alkyls.

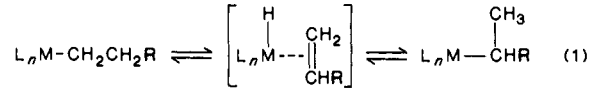

In the skeletal isomerization of transition-metal alkyls isomerization from *sec*-alkyl to *n*-alkyl has been often observed, a process favored by the steric bulkiness of the coordinated ligand. Such isomerization processes are important in catalytic processes such as hydroformylation for producing a linear chain product. For metallacycles, however, such isomerizations have been reported in very limited cases. Whitesides[8] and Schrock[9] suggested oc-

(1) Cotton, F. A.; Wilkinson, G. *Advanced Inorganic Chemistry*; Interscience: New York, 1972; p 785-793.
(2) Heck, R. *Organotransition Metal Chemistry*; Academic Press: New York, 1974; p 206-207.
(3) (a) Collman, J. P.; Hegedus, L. S. *Principles and Applications of Organotransition Metal Chemistry*; University Science Books: Mill Valley, CA, 1980; p 571.
(4) Bennett, M. A.; Charles, R. *J. Am. Chem. Soc.* **1972**, *94*, 666-667.
(5) (a) Kiso, Y.; Tamao, K.; Kumada, M. *J. Organomet. Chem.* **1973**, *50*, C12-C14. (b) Komiya, S.; Morimoto, Y.; Yamamoto, A.; Yamamoto, T. *Organometallics* **1982**, *1*, 1528.
(6) Reger, D. L.; Culbertson, E. C. *Inorg. Chem.* **1977**, *16*, 3104-3107.
(7) Tamaki, A.; Kochi, J. K. *J. Chem. Soc., Chem. Commun.* **1973**, 423-424.

(8) Young, G. B.; Whitesides, G. M. *J. Am. Chem. Soc.* **1978**, *100*, 5808-5815.

0002-7863/87/1509-1092$01.50/0

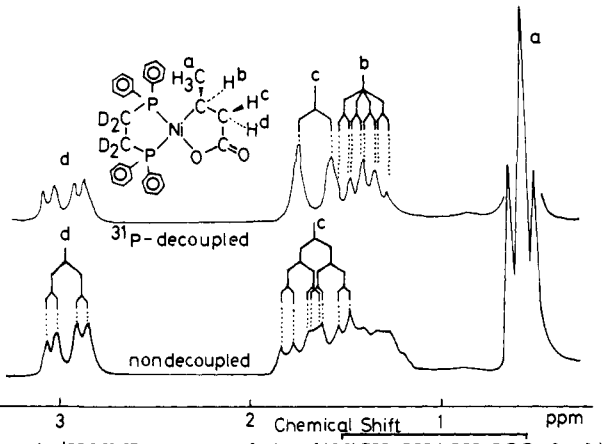

Figure 1. ^1H NMR spectrum of (dpe-d_4)NiCH(CH$_3$)CH$_2$COO (**2a**-d_4) in CD_2Cl_2 at 24 °C (100 MHz). The triplet of H^a becomes a doublet after the ^{31}P decompling.

currence of ring contraction in thermolysis of platina- and tantalacycles, but no product has been isolated in the presumed ring contraction reactions.

In the course of our investigation on reactivities of transition-metal-containing cyclic esters,[10-13] we have found ring contraction reaction of six-membered nickel-containing cyclic esters, the process converting an *n*-alkyl group in the six-membered ring complex into a *sec*-alkyl group. By formation of the methyl-substituted nickel-containing cyclic ester, **2**, a chiral center as

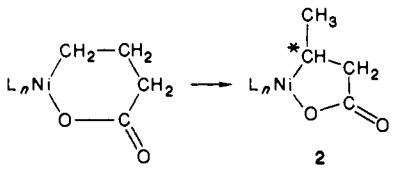

(2)

1 **2**

marked by * is generated at the secondary α-carbon bonded to Ni, and use of a chiral diphosphine ligand is expected to induce formation of unequal amounts of diastereomers. By finding the ring contraction reaction the following questions emerged. (1) What factors control the ring contraction reaction? (2) If use of the chiral diphosphine actually leads to formation of the diastereomers in unequal amounts, what is the effect of the chiral phosphine on the distribution of the diastereomers? (3) How are the ring contraction reaction and asymmetric induction explained on the basis of molecular structures of **1** and **2**?

We now report results of our research attempting to answer these questions. Part of the results in this paper were briefly reported in communication form.[13,14]

Results and Discussion

Ring Contraction. When a six-membered ring complex (dpe)NiCH$_2$CH$_2$CH$_2$COO (**1a**), which is prepared in a heterogeneous reaction system,[12,13] is dissolved in solutions, instant ring contraction of **1a** to a five-membered ring complex, (dpe)-NiCH(CH$_3$)CH$_2$COO (**2a**), takes place.

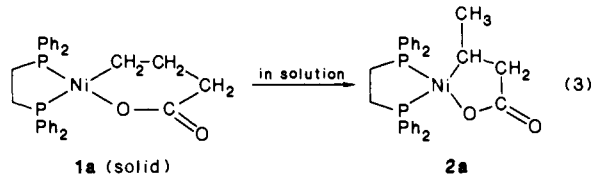

(3)

1a (solid) **2a**

(bpy)NiCH$_2$CH$_2$CH$_2$COO (**1b**, bpy = 2,2′-bipyridine)[12] maintains its six-membered ring structure both in the solid state and in solutions. However, addition of 1,2-bis(diphenylphosphino)ethane (dpe) to the solution of **1b** causes rapid replacement[15] of the bpy ligand by dpe and brings about the rapid ring contraction to give (dpe)NiCH(CH$_3$)CH$_2$COO (**2a**). By

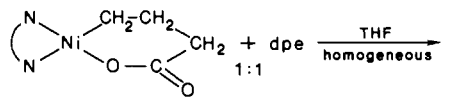

1b

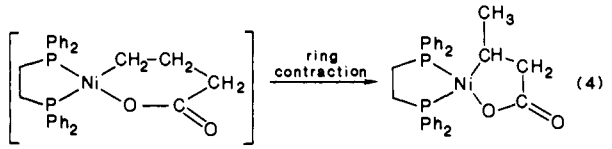

(4)

1a **2a**

using dpe-d_4 ($Ph_2PCD_2CD_2PPh_2$) we prepared **2a**-d_4 for obtaining clear-cut information on NMR spectra of the dpe-coordinated complex. Figure 1 shows ^1H NMR and $^1H\{^{31}P\}$ NMR spectra of **2a**-d_4. The nondecoupled as well as homodecoupled spectra of **2a**-d_4 support the structure of **2a** as indicated in the figure. $^{13}C\{^1H\}$ and $^{31}P\{^1H\}$ NMR spectra as well as elemental analytical data are also consistent with the structure of **2a**. The ν(C=O) band of **2a** (1640 cm^{-1}) appears at a higher frequency than those of **1a** and **1b** by 40 and 20 cm^{-1}, respectively, in accord with a general trend that a five-membered cyclic ester shows a ν(C=O) band at higher frequency than six-membered cyclic ester.[16]

Complex **2a** reacts with carbon monoxide to give 3-methylsuccinic anhydride, whereas the reaction of **1a** with CO affords glutaric anhydride. The heterogeneity of the reaction system of

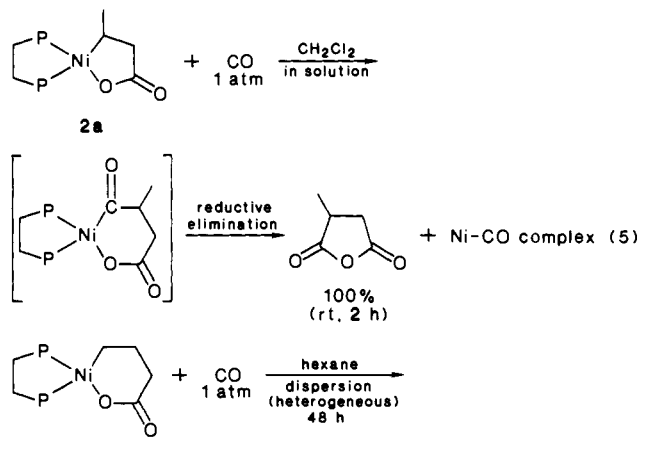

2a

1a (solid)

glutaric anhydride 41% (rt, 48 h) + Ni-CO complex +

3-methylsuccinic anhydride (8%) (6)

eq 6 accounts for the relatively low yield of glutaric anhydride in eq 6, and the partial formation of 3-methylsuccinic anhydride seems to be due to isomerization of **1a** during the reaction with CO.

(9) McLain, S. J.; Sancho, J.; Schrock, R. R. *J. Am. Chem. Soc.* **1979**, *101*, 5451-5453.

(10) Yamamoto, T.; Igarashi, K.; Komiya, S.; Yamamoto, A. *J. Am. Chem. Soc.* **1980**, *102*, 7338-7456.

(11) Sano, K.; Yamamoto, T.; Yamamoto, A. *Chem. Lett.* **1983**, 115-118.

(12) Sano, K.; Yamamoto, T.; Yamamoto, A. *Bull. Chem. Soc. Jpn.* **1984**, *57*, 2741-2747. The ^{1}NMR (^1H, $^{13}C\{^1H\}$, $^{31}P\{^1H\}$) data of **2a** (**5** in this reference) and those of (dpe)NiCH$_2$CH(CH$_3$)COO (**8** in this reference) were exchanged in Table II of this reference by mistake. The NMR data of **2a** given in ref 13 are correct.

(13) Sano, K.; Yamamoto, T.; Yamamoto, A. *Chem. Lett.* **1982**, 695-698. Ring contraction of a seven-membered nickelacyclic compound to a six-membered nickelacyclic compound was assumed in a recently reported catalytic reaction by using Ni(0) complexes (Hoberg, H.; Hernandez, E. *J. Chem. Soc., Chem. Commun.* **1986**, 544-545).

(14) Sano, K.; Yamamoto, T.; Yamamoto, A. *Chem. Lett.* **1984**, 941-944.

(15) Much higher coordinating ability of dpe to an organonickel complex than that of bpy has been reported (Kohara, T.; Yamamoto, T.; Yamamoto, A. *J. Organomet. Chem.* **1980**, *192*, 265-274).

(16) Pouchart, C. J. *The Adrich Library of Infrared Spectra*; Aldrich: St. Paul, 1975; p 360-366.

Table I. Effect of Added Ligand on the Ring Contraction Reaction. Ratio between Glutaric Anhydride and 3-Methylsuccinic Anhydride Obtained on Treatment of the Reaction Mixture (Equations 8 and 9) with CO[a]

							product[e] (% yield/Ni)	
no.	ligand[b]	cone angle[c] (deg)	pK_a[d]	ligand/Ni	temp (°C)	time (h)	glutaric anhydride	3-methylsuccinic anhydride
1	PMe_2Ph	122	7.9	2	10	1	52	trace
2	PEt_3	132	8.7	1	10	1	66	trace
3	PEt_3			2	10	1	47	9
4	PEt_3			2	10	3	58	20
5	PEt_3			2	10	24	29	47
6	PEt_3			4	10	1	25	44
7	PEt_3			2	30	1	32	42
8	PBu_3	132	8.4	2	10	1	46	3
9	$PMePh_2$	136	5.4	2	10	1	59	9
10	PEt_2Ph	136	6.8	2	10	1	66	9
11	$PEtPh_2$	140	5.4	2	10	1	66	4
12	PPh_3	145	3.2	2	10	1	70	trace
13	dmpe[b]			1	10	1	44	5

[a] The mixture of $Ni(cod)_2$, glutaric anhydride (1 mol/mol of $Ni(cod)_2$), and ligand was stirred at the temperature and for the period given in this table (solvent = THF). After that CO (1 atm) was introduced into the reaction mixture at ca. 25 °C, and the system was kept for half an hour. [b] dmpe = 1,2-bis(dimethylphosphino)ethane. [c] See the text. [d] pK_a of the conjugate acid of the ligand. [e] Yield of glutaric anhydride = (glutaric anhydride after the treatment with CO) − (glutaric anhydride before treatment with CO); see Experimental Section.

Addition of 1,3-bis(diphenylphosphino)propane (dpp) to a CH_2Cl_2 solution of **1b** also induces a rapid ring contraction. Further reaction of the ligand-exchanged product with CO gives 3-methylsuccinic anhydride exclusively. These results clearly indicate that the coordination of diphosphine ligands induces the ring contraction.

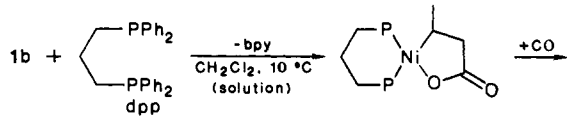

3-methylsuccinic anhydride (41%/Ni) (7)

Effect of Ligand on the Ring Contraction. As shown above, stability of the six-membered ring in $L_nNiCH_2CH_2CH_2COO$ is strongly influenced by the auxiliary ligand L (e.g., bpy and dpe). In order to reveal the effect of the ligand on the ring contraction reaction, we carried out reactions of $Ni(cod)_2$ (cod = 1,5-cyclooctadiene) with glutaric anhydride in the presence of various ligands. Reactions shown in eq 8 were employed to prepare the

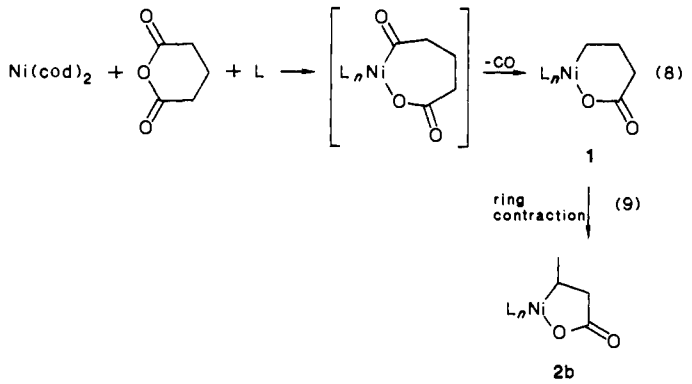

nickel-containing cyclic ester type complexes,[12,17] and **1b** was actually prepared by using the reaction.[12] Treatment of the reaction mixture with CO, giving glutaric anhydride from **1** and 3-methylsuccinic anhydride from **2**, provides information about the extent of the ring contraction (eq 9) that occurred in the reaction system. Table I shows yields of glutaric anhydride and

$$\mathbf{1} + CO \rightarrow \text{glutaric anhydride} \quad (10)$$

$$\mathbf{2b} + CO \rightarrow \text{3-methylsuccinic anhydride} \quad (11)$$

3-methylsuccinic anhydride formed in the reaction of CO with the reaction product obtained by mixing $Ni(cod)_2$, glutaric anhydride, and L (eq 8 and 9). The yield of 3-methylsuccinic anhydride relative to glutaric anhydride recovered from the reaction mixtures may be taken as a measure of degree of the ring contraction that occurred in eq 9.[18] From examination of the results shown in Table I and above the following features are seen. (1) Data shown in no. 2, 3, and 6 (Table I) indicate that addition of more than 2 mol of PEt_3 per $Ni(cod)_2$ is necessary to induce the ring contraction, suggesting that the ring contraction proceeds in four coordinate $L_2NiCH_2CH_2CH_2COO$ type complexes[19] when L is the monodentate ligand. (2) The degree of the ring contraction increases with time (no. 3–5), and the rate of ring contraction increases with raising the reaction temperature (no. 3 and 7). (3) There seems to be a trend that coordination of more sterically demanding ligand to nickel facilitates the ring contraction.

Comparison of the degrees of the ring contraction in the bidentate ligand-coordinated complexes, $(L\text{–}L)NiCH_2CH_2CH_2COO$, and bulkiness of the ligand reveals the following trend.

bidentate ligand	bulkiness	deg of ring contraction
bpy	flat and not bulky	none
dmpe	medium	medium
dpe	bulky	100%

A similar trend is also seen for the complexes with monodentate phosphines. Addition of PMe_2Ph (Tolman's cone angle[20] θ = 122°, no. 1 in Table I) caused only a small extent of ring contraction. On the other hand, coordination of PEt_3 (θ = 132°, no. 3) demands larger space and in this case degree of the ring contraction is larger. Use of PBu_3, $PMePh_2$, PEt_2Ph, and $PEtPh_2$ (no. 8–11) having the cone angle ranging from 132–140° affords analogous results. In cases of PPh_3 (no. 12) and PCy_3 having the cone angle of larger than 145°, the CPK molecular model indicates that coordination

(17) Uhlig, V. E.; Fenske, G.; Nestler, B. *Z. Anorg. Allg. Chem.* **1980**, *465*, 141–146.

(18) Reaction of the bpy coordinated complex **1b** with ligands and treatment of the reaction mixture with CO (cf. eq 4 and 5) may afford more direct information concerning the effect of ligand on the ring contraction. However, use of some monodentate ligands seems not to cause such the complete ligand exchange as that observed on addition of dpe and dpp to **1b**, and under these circumstances treatment of the reaction mixture with CO may give misleading information concerning the effect of ligand on the ring contraction. Therefore, we carried out reactions 8–11 to estimate the effect of the ligand.

(19) Addition of PEt_3 (ca. 2 mol/Ni) to an analogous nickelacyclic compound $[(PEt_3)NiCH_2C(CH_3)CONH]_n$[10] in THF-$d_8$ affords $(PEt_3)_2NiCH_2C(CH_3)CONH$ quantitatively as proved by observing the ^{31}P NMR spectrum of the mixture, which shows two doublets at 36.61 ($J(^{31}P\text{–}^{31}P)$ = 22.0 Hz) and 48.14 ppm, respectively, downfield from free PEt_3 (in THF-d_8 at −78 °C).

(20) Tolman, C. A. *Chem. Rev.* **1977**, *77*, 313–348.

of two molecules of these phosphine ligands to $\overline{NiCH_2CH_2CH_2COO}$ is very difficult.

Complex **3a** having a six-membered metallacycle with a β-CH_3 group has been prepared in situ according to the following equation. This complex did not give the ring contracted complex despite of its being a six-membered metallacycle. Treatment of

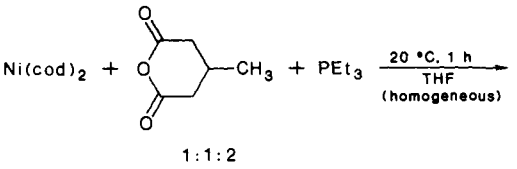

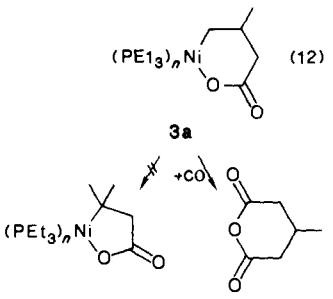

(12)

the reaction product with CO gives 4-methylglutaric anhydride exclusively, indicating that the β-elimination does not proceed in a complex such as **3a** having the methyl substituent at the β-carbon. Another six-membered metallacycle having the methyl substituent at the β-carbon, i.e., dpe-coordinated complex (**3c**) (eq 13) did not undergo the ring contraction, either. These results suggest that the ring contraction which most probably proceeds through the β-elimination process is hindered by the substitution at the β-carbon.

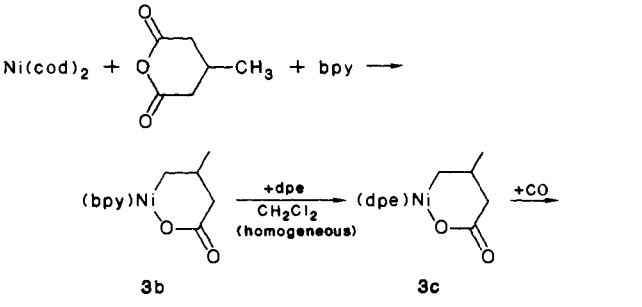

4-methylglutaric anhydride (60%) (13)

We have also examined the possibility of a ring expansion of complex **2** to complex **1**, the reverse reaction of the ring contraction reaction, under various reaction conditions. However, no ring expansion was found, the result indicating that the five-membered ring in **2** is more stable than the six-membered ring in **1** despite that complexes with the branched alkyl chains are usually less stable than those having the *n*-alkyl groups.

Asymmetric Induction in the Ring Contraction. Use of chiral tetraaryldiphosphines such (*S*,*S*)-chiraphos and (*R*,*R*)-dipamp as ligands affords homogeneous transition-metal (e.g., rhodium) catalysts suitable for asymmetric hydrogenation of prochiral olefins.[21,22] It is now recognized that the edge-face array of the aryl rings of the chiral diphosphines around metals is the controlling factor of the configuration of the hydrogenated product.

In order to examine how the edge-face array of the aryl rings of the chiral diphosphine determines the configuration of the present ring contracted complex **2**, we added the following chiral diphosphines to a homogeneous solution of the six-membered complex **1b**.

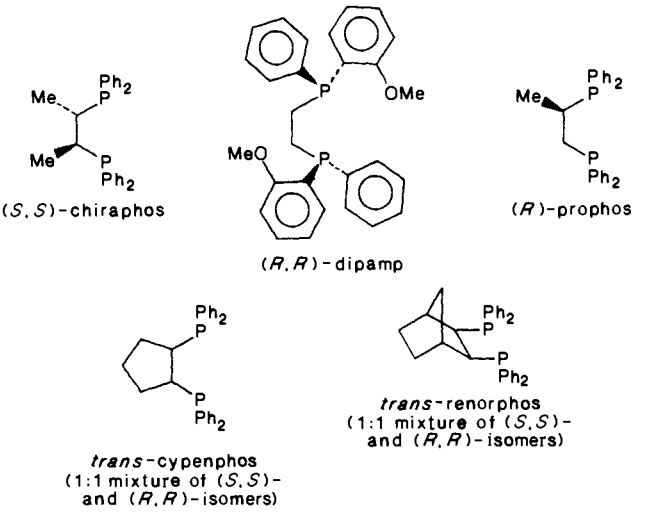

Addition of the diphosphines to **1b** caused instant ring contraction as proved by the NMR (^1H, $^{31}P\{^1H\}$, and $^{13}C\{^1H\}$) and IR spectra of the compounds recovered after addition of the diphosphines. The product was revealed to be mixtures of two diastereomers having R and S configurations, respectively, at the α-carbon in the five-membered nickel-containing cyclic ester unit, (***R***)-**2** and (***S***)-**2**.

If the present ring contraction proceeds through the β-elimination mechanism (eq 14b), the postulated intermediate **4a** likely has a quasifive-membered ring structure by coordination of the

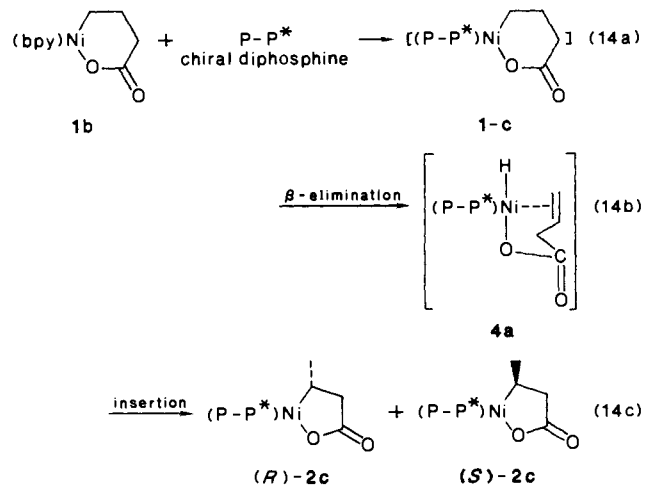

(14a) (14b) (14c)

C=C double bond to nickel. The quasifive-membered structure around nickel in **4a** is reminiscent of a quasifive-membered ring structure around rhodium in **5** which has been proposed as an

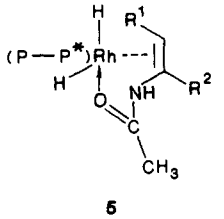

5

active intermediate for asymmetric synthesis of α-amino acid derivatives.[21,22] As described above, the configuration of α-amino acid derivatives formed is considered to be determined by the edge-face array of the aryl rings of P–P* in **5**.[21,22]

Use of (*S*,*S*)-Chiraphos as the Chiral Diphosphine. The $^{31}P\{^1H\}$ NMR spectrum observed immediately after addition of (*S*,*S*)-

(21) (a) Halpern, J. *Science*, **1982**, *217*, 401–407. Halpern, J. *Pure Appl. Chem.* **1983**, *55*, 99–106. (b) Brown, J. M.; Chaloner, P. A.; Parker, D. *Catalytic Aspects of Metal Phosphine Complexes*; Alyea, E. C., Meek, D. W., Eds.; American Chemical Society: Washington, DC, 1982; 355–369.

(22) (a) Knowles, W. S.; Vineyard, B. D.; Sabacky, M. J.; Stuls, B. R. *Fundamental Research in Homogeneous Catalysis*; Tsutsui, M., ed.; Plenum Press: New York, 1980; pp 537–548. (b) Bosnich, B.; Roberts, N. K. *Catalytic Aspects of Metal Phosphine Complexes*; Alyea, E. C., Meek, D. W., Eds.; American Chemical Society: Washington, DC, 1982; pp 337–354. (c) Fryzuk, M. D.; Bosnich, B. *J. Am. Chem. Soc.* **1977**, *99*, 6262–6267. (d) Ball, R. G.; Payne, N. C. *Inorg. Chem.* **1977**, *16*, 1187–1191.

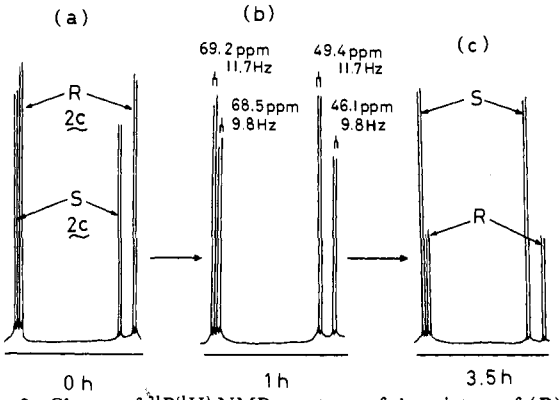

Figure 2. Change of $^{31}P\{^1H\}$ NMR spectrum of the mixture of (***R***)-**2c** and (***S***)-**2c** prepared by mixing **1b** and (*S*,*S*)-chiraphos with time (40 MHz, 24 °C).

chiraphos to **1b** (Figure 2a) shows two sets of two doublets arising from the following two diastereomers ***R***-**2c** and ***S***-**2c**. For assignment of the configuration, complex (***R***)-**2c** was independently prepared through the reaction of (*R*)-methylsuccinic anhydride (100% ee) with a zero valent nickel complex.[12] Reaction 16a proceeds via ring opening of 3-methylsuccinic anhydride and the subsequent decarbonylation processes which most probably proceed with stereochemical retention at the methyl-substituted carbon.[24]

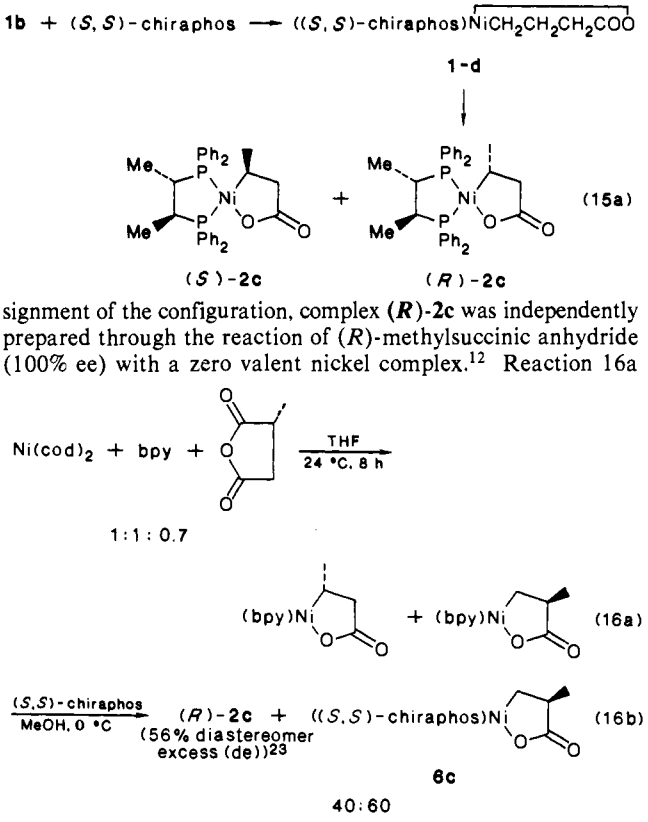

Table II. $^{31}P\{^1H\}$ NMR Data of (P–P)NiCH(CH$_3$)CH$_2$COO and Related Complexes[a]

P–P	complex	solvent[b]	chemical shift[c] ppm		J(P–P′) Hz
dpe	**2a**	A	63.2	41.2	9.8
	2a	B	63.5	42.1	9.8
(*S*,*S*)-chiraphos	(*R*)-**2c**	A	68.5	46.1	9.8
	(*R*)-**2c**	B	68.9	46.2	9.8
	(*S*)-**2c**	A	69.2	49.4	11.7
	(*S*)-**2c**	B	68.7	50.5	11.7
(*R*,*R*)-dipamp	(*R*)-**2d**	A	59.6	41.0	7.8
	(*S*)-**2d**	A	58.9	38.3	7.8
(*R*)-prophos	(*R*)-*cis*-**2e**	A	69.4	30.7 (Δ = 38.7)	5.9
	(*R*)-*trans*-**2e**	A	55.8	51.0 (Δ = 4.7)	2.0
	(*S*)-*cis*-**2e**	A	68.7	29.5 (Δ = 39.2)	2.9
	(*S*)-*trans*-**2e**	A	59.7	55.7 (Δ = 4.0)	10.7
trans-cypenphos	**2f** diastermr α's	A	46.8	21.5	15.1
	2f diastermr β's	A	48.3	24.6	14.6
trans-renorphos	**2g** diastermr-α or γ's (set a)	A	37.8	20.0 (Δ = 17.8)	16.6
	2g diastermr-β or δ's (set b)	A	40.2	24.1 (Δ = 16.1)	16.6
	2g diastermr-γ or α's (set c)	A	46.4	11.1 (Δ = 35.3)	18.6
	2g diastermr-δ or β's (set d)	A	48.6	14.6 (Δ = 34.0)	18.6
(*S*,*S*)-chiraphos	**6c**	A	70.5	47.2	20.5
(*R*,*R*)-dipamp	**6d**	A	59.6	37.7	ca. 0
(*R*)-prophos	*cis*- or *trans*-**6e**	A	71.7	31.3	7.8
	cis- or *trans*-**6e**	A	60.5	53.3	ca. 0
	Ni(dpe)$_2$	A	49.0		

[a] 40 MHz at 24 °C. [b] Methanol plus a small amount of acetone-d_6 for A; CD_2Cl_2 for B. [c] Downfield positive from external PPh_3.

The $^{31}P\{^1H\}$ NMR spectrum (Figure 2) shows that (***R***)-**2c** which is present in 12–16% diastereomer excess (de)[25] in the beginning decreases with reversal of its configuration eventually to give (***S***)-**2c** in 54% de after 10 h at 24 °C, demonstrating that the kinetically favored diastereomer, (***R***)-**2c**, is transformed into the thermodynamically favored diastereomer, (***S***)-**2c**, in the present system. The present finding represents the first example, to our knowledge, of observation of configurational reversal from the kinetically controlled chiral alkyl complex to the thermodynamically controlled chiral alkyl complex of the opposite configuration. Table II summarizes ^{31}P NMR data of **2** and the related complex.

Figure 3 shows time course of the *R* to *S* isomerization of **2c** in methyl alcohol at various temperatures. The isomerization between (***R***)-**2c** and (***S***)-**2c** obeys first-order kinetics, with rate constants of 1.2×10^{-4} s^{-1} (k_1) and 3.6×10^{-5} s^{-1} (k_{-1}) at 24 °C for the forward and backward reactions. From the temperature

$$(R)\text{-}\mathbf{2c} \underset{k_{-1}}{\overset{k_1}{\rightleftharpoons}} (S)\text{-}\mathbf{2c} \qquad (17)$$

dependence of the k_1 values, the kinetic parameters for the *R* to *S* isomerization have been calculated as $\Delta H_1^{\ddagger} = 93 \pm 2$ kJ mol^{-1}, $\Delta S_1^{\ddagger} = -8 \pm 6$ J mol^{-1} K^{-1}, and $\Delta G_1^{\ddagger} = 95$ kJ mol^{-1} at 24 °C (Table III). From the temperature dependence of the equilibrium constant, $K = k_1/k_{-1}$, the thermodynamic parameters for the equilibrium have been obtained as follows: $\Delta H° = 13 \pm 2$ kJ mol^{-1}, $\Delta S° = 54 \pm 6$ J mol^{-1} K^{-1}, and $\Delta G° = -3.0$ kJ mol^{-1} at 24 °C.

The *R* to *S* isomerization of complex **2c** in other various solvents including acetone, CH_3CN, THF, and pyridine also obeys the first-order kinetics, and the de values observed in these solvents after equilibration are roughly the same as that observed in methyl

(23) The $^{31}P\{^1H\}$ NMR spectrum of the reaction mixture obtained under conditions given in eq 16 shows two sets of two doublets at the same positions with those shown in Figure 2. Besides the two sets of doublets, the NMR spectrum shows two doublets assignable to **6c** (not shown in the figure). The de value of (***R***)-**2c** estimated from the $^{31}P\{^1H\}$ NMR spectrum observed immediately after (time to take $^{31}P\{^1H\}$ NMR spectrum = ca. 30 min[25]) addition of S,S-chiraphos (eq 16b) was 56%. However, when the reaction mixture was allowed to stand at 24 °C for 50 min, the de value decreased to 12%, and after 5 h the (***S***)-**2c** isomer became the major species due to the (*R*) → (*S*) isomerization described in the text.

(24) Decarbonylation from acyliron complexes is reported to proceed with stereochemical retention. (a) Walborsky, H. M.; Allen, L. E. *J. Am. Chem. Soc.* **1971**, *93*, 5465–5468. (b) Lock, P. L.; Boschetto, D. J.; Rasmussen, J. R.; Demers, J. P.; Whitesides, G. M. *J. Am. Chem. Soc.* **1974**, *96*, 2814–2825. Its reverse type-reaction, carbonylation of alkyltransition-metal complex, is also reported to proceed with stereochemical retention. (c) Stille, J. K.; Hines, L. F. *J. Am. Chem. Soc.* **1970**, *92*, 1798–1799. (d) Flood, T. C. *Topics in Inorganic and Organometallic Stereochemistry*; Geoffroy, G. L., Ed.; John Wiley: New York, 1981; Vol. 12, pp 83–85. (e) Kuhlmann, E. J.; Alexander, J. J. *Coord. Chem. Rev.* **1980**, *33*, 195–225.

(25) Since it takes 0.5–1 h for measuring the first ^{31}P NMR spectrum of **2c** prepared by mixing **1b** with (*S*,*S*)-chiraphos, the initial de of **2c** is considered to be higher than 16%.

Table III. The First-Order Rate Constant for Configurational Isomerization of (*R*)-**2** to (*S*)-**2** or (*S*)-**2** to (*R*)-**2**

complex	type of isomerztn[a]	solvent	temp (K)	k_1 (10^{-4} s^{-1})	k_{-1} (10^{-4} s^{-1})	$K = k_1/k_{-1}$		de after equilbrtn
2c	R→S	MeOH	283	0.16[b]	0.062	2.6	$\Delta H°$ = 13 ± 2 kJ/mol	44 (*S*)
			297	1.2[b]	0.36	3.3	$\Delta S°$ = 54 ± 6 J/(mol K)	54 (*S*)
			308	3.7[b]	0.92	4.0	$\Delta G°$ = −3.0 kJ/mol	60 (*S*)
		acetone	297	1.2	0.44	2.7		46 (*S*)
		CH_3CN	297	0.82	0.34	2.4		42 (*S*)
		CH_2Cl_2	297	0.71	0.18	4.0		60 (*S*)
		THF	297	0.52	0.15	3.5		56 (*S*)
		pyridine	297	0.47	0.13	3.5		56 (*S*)
2d	S→R	MeOH	297	ca. 0.4	ca. 0.13	3.0		50 (*R*)
cis-**2e**		MeOH	283					49 (*R*)
			293					53 (*R*)
			303					54 (*R*)
trans-**2e**		MeOH	283					42 (*S*)
			293					34 (*S*)
			303					26 (*S*)
2f	diastermr-α → diastermr-β	MeOH	297	1.5	0.58	2.7		46
2g	diastermr-α → diastermr-β	MeOH	297	1.3	0.11	11.5		84
	or				or			or
	diastermr-γ → diastermr-δ			1.1	0.16	6.7		74

[a] Assignments of configurations of **2e**, **2f**, and **2g** are tentative (see the text). [b] $\Delta H_1^{\ddagger}$ = 93 ± 2 kJ mol^{-1}, $\Delta S_1^{\ddagger}$ = −8 ± 6 J mol^{-1} K^{-1}, $\Delta G_1^{\ddagger}$ = 95 kJ mol^{-1}.

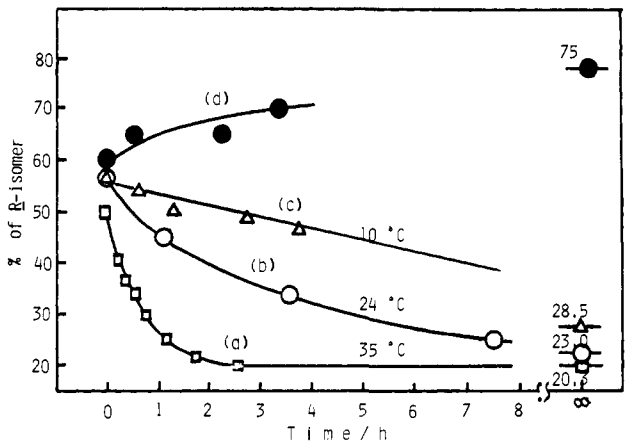

Figure 3. Time course of *R* to *S* isomerization of **2c** at 35 °C (□), 24 °C (○), and 10 °C (△) and time course of *S* to *R* isomerization of **2d** at 24 °C (●) (solvent = methanol).

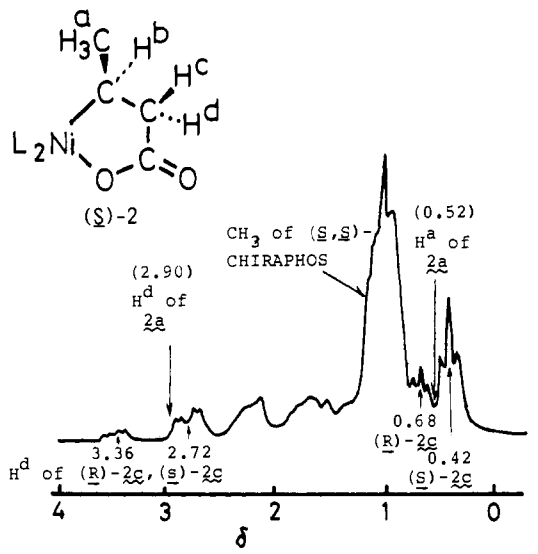

Figure 4. ^1H NMR spectrum of the mixture of (***R***)-**2c**, and (***S***)-**2c** in CD_2Cl_2 after attainment of equilibrium at 24 °C (100 MHz).

alcohol. Data of the *R* to *S* isomerization of **2c** are summarized in Table III together with results obtained for similar *R* to *S* or *S* to *R* isomerizations of other complexes. The $^{31}P\{^1H\}$ NMR signals of (***R***)-**2c** and (***S***)-**2c** in solvents other than methyl alcohol are observed at almost the same positions as those of signals shown in Figure 2.

Figure 4 shows the ^1H NMR spectrum of the mixture of (***R***)-**2c** and (***S***)-**2c** after attainment of equilibrium at 24 °C. The figure shows two triplets at δ 0.68 and 0.42 ppm which are assigned to the α-CH_3 protons of (***R***)-**2c** and (***S***)-**2c**, respectively. The two quartets at δ 3.36 and 2.72 ppm are assigned to one of the β-methylene protons (cf. H^d in Figure 1) of (***R***)-**2c** and (***S***)-**2c**, respectively. It is noted that the triplet of the α-CH_3 protons of the dpe-coordinated complex **2a** (δ 0.52 ppm) has been observed in Figure 1 at the middle of the two triplets of the α-CH_3 protons of (***R***)-**2c** and (***S***)-**2c**. A similar relation holds between signals of H^d of **2a** and of the pair of (***R***)-**2c** and (***S***)-**2c**. The CPK molecular models of (***R***)-**2c** and (***S***)-**2c** indicate as shown in Figure 5 that the α-CH_3 protons in (***S***)-**2c** are located at the face position of the phenyl ring of (*S*,*S*)-chiraphos, whereas those protons in (***R***)-**2c** are located at the edge position of the phenyl ring if (*S*,*S*)-chiraphos in **2c** takes δ-conformation[21,22] (vide infra). The observation of chemical shifts of the α-CH_3 protons of (***S***)-**2c** at higher magnetic field than those of (***R***)-**2c** is consistent with the assumption that they are located in the region close to the face of the phenyl ring. These results suggest that the (*S*,*S*)-chiraphos in **2c** takes only one rigid conformation (presumably δ), whereas the dpe in **2a** can take both δ and λ conformations,

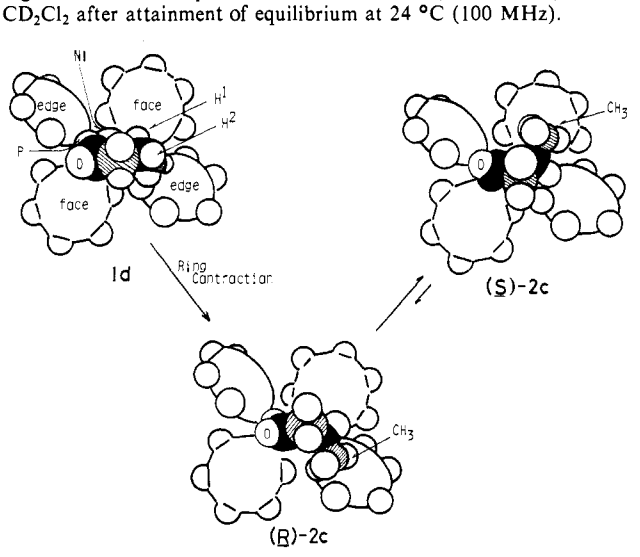

Figure 5. Sketch of CPK molecular models of **1d**, (***R***)-**2c**, and (***S***)-**2c**. For **1d**, Cα and Cγ are hatched. Cβ and C=O carbon are black. For Cα, Cβ, Cγ, H^1, and H^2, see eq 18.

and exchange between the two conformations is very rapid on the NMR time scale. The rapid exchange did not freeze at −80 °C.

Molecular Model for the Asymmetric Induction and the *R* to *S* Isomerization of 2c. We now try to elucidate the results of the asymmetric induction and the *R* to *S* isomerization of **2c** by using molecular models for the initial six-membered complex **1d** (eq 15a) and the ring-contracted complexes, (*R*)-**2c** and (*S*)-**2c**. Figure 5 shows the CPK molecular models of the complexes. If the coordinating (*S*,*S*)-chiraphos takes a δ-conformation as observed in a rhodium complex,[21,22] the CPK molecular model of **1d** suggests that the six-membered cyclic ester ring prefers the λ-conformation[26] where one (H^1) of the two β-hydrogens is situated at a closer distance than the other hydrogen atom (H^2) to the nickel atom to be preferentially abstracted.

Abstraction of H^1 by Ni and reinsertion in **4a** before rotation around the Cβ–Cγ bond leads to the formation of (*R*)-**2c**. Complex (*R*)-**2c** thus formed, however, is less stable than (*S*)-**2c**.

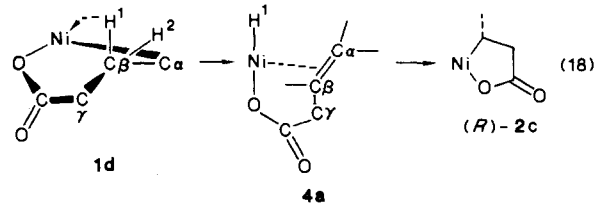

The CPK molecular model of (*R*)-**2c** shows presence of steric repulsion between the α-CH_3 group and an edge phenyl group of (*S*,*S*)-chiraphos coordinated to Ni (Figure 5). Due to the steric repulsion, rotation of the CH_3 group of the five-membered cyclic ester group around the C–CH_3 bond as well as other intramolecular movement in (*R*)-**2c** is hindered. In (*S*)-**2c**, on the other hand, the α-CH_3 group avoids the repulsion by the edge-phenyl group, and free rotation of the CH_3 group is allowed. Thus (*S*)-**2c** is thermodynamically more stable than (*R*)-**2c**, the kinetic product. This reasoning is consistent with the observed positive ΔS value for the *R* to *S* isomerization of **2c**. The steric repulsion between the α-CH_3 group and the edge phenyl group in (*R*)-**2c** implies a negative ΔH value for the *R* to *S* isomerization. The observed ΔH, however, has a positive value, and this suggests that other unrevealed intermolecular or intramolecular interactions are more important to determine the ΔH value. For example, the *R* to *S* isomerization will cause change in dipole and/or quadrupole moment of **2c**, thus leading to change in strength of interaction of **2c** with solvent.

Use of Other Chiral Diphosphines. (*R*,*R*)-Dipamp. When (*R*,*R*)-dipamp which is known to prefer the conformation (λ) opposite to (*S*,*S*)-chiraphos[21,22] is employed, an opposite result to that obtained with (*S*,*S*)-chiraphos is obtained. $^{31}P\{^1H\}$ NMR spectrum of a mixture of **1b** and (*R*,*R*)-dipamp shows two sets of two doublets indicating formation of the following two diastereomers, (*R*)-**2d** and (*S*)-**2d**.

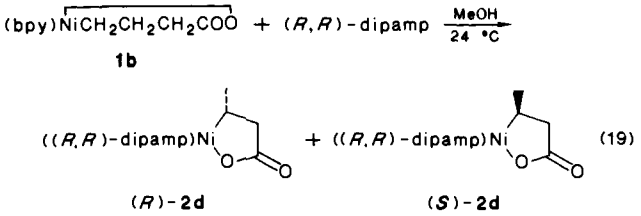

Signals of (*R*)-**2d** have been assigned by comparing the $^{31}P\{^1H\}$ NMR spectrum of the mixture of (*R*)- and (*S*)-**2d** with a $^{31}P\{^1H\}$ NMR spectrum of the reaction mixture obtained by mixing $Ni(cod)_2$ and (*R*)-3-methylsuccinic anhydride in the presence of bpy and ensuing addition of (*R*,*R*)-dipamp. The system is considered to give a mixture of (*R*)-**2d** and ((*R*,*R*)-dipamp)-(*R*)-$NiCH_2CH(CH_3)COO$, **6d**, by a process similar to that shown in eq 16 (Table II).

(26) The δ and λ conformations concerning the six-membered ring in **1d** are defined by the direction of torsion of a line connecting the β and C=O carbons (cf. eq 18) from the molecular plane.

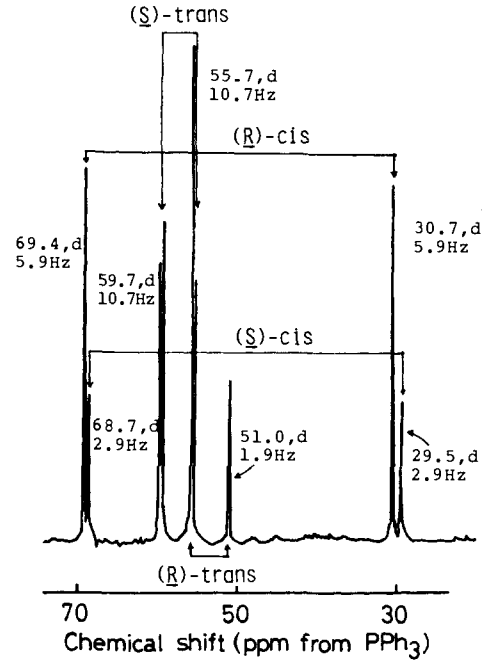

Figure 6. $^{31}P\{^1H\}$ NMR spectrum of a mixture of (*R*)-**2e** and (*S*)-**2e** in methyl alcohol at 24 °C. In this figure, signals other than the signals of (*S*)-*trans*-**2e** look singlets. However, an expanded spectrum reveals that all signals are doublet (Table II).

The thermodynamically equilibriated mixture of the (*R*,*R*)-dipamp complexes after the ring contraction at 24 °C contains the (*R*)-isomer in 50% de (Figure 3) in contrast to the result obtained with (*S*,*S*)-chiraphos. The initial product obtained immediately after the ring contraction, however, contains more amount of (*S*)-**2d** than the equilibriated product, and the isomerization from (*S*)-**2d** to (*R*)-**2d** roughly obeys first-order kinetics with a rate constant of 5.5×10^{-5} s^{-1} at 24 °C.

(*R*)-Prophos. Similarly to the cases of (*S*,*S*)-chiraphos and (*R*,*R*)-dipamp, a mixture of (*R*)-**2e** and (*S*)-**2e** is obtained by the following reaction

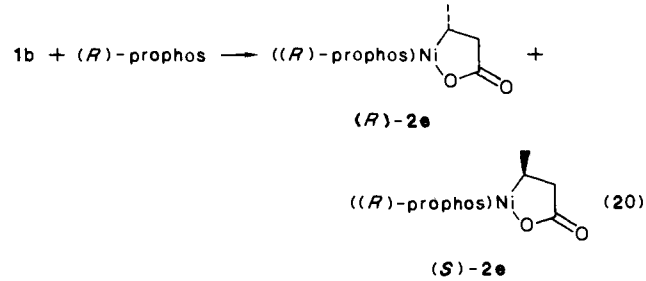

By using (*R*)-3-methylsuccinic anhydride, we prepared (*R*)-**2e** as in the cases of (*R*)-**2c** (eq 16) and (*R*)-**2d** and thus assigned the $^{31}P\{^1H\}$ signals of (*R*)-**2e**. The $^{31}P\{^1H\}$ NMR spectrum (Figure 6) of the mixture of (*R*)- and (*S*)-**2e**, however, is complicated by the presence of cis and trans isomers of (*R*)- and (*S*)-**2e**, and the spectrum shows four sets of two doublets. We tentatively assign

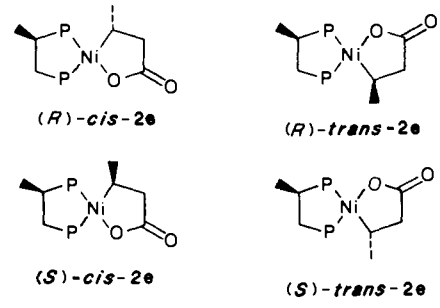

the $^{31}P\{^1H\}$ NMR signals as shown in Figure 6 and Table II on

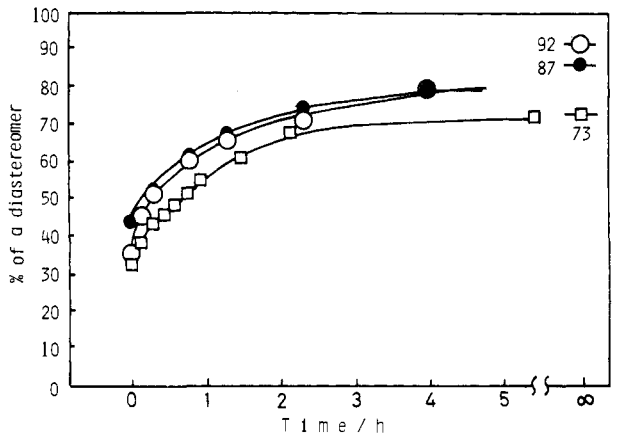

Figure 7. Change of distribution of diastereomers with time at 24 °C in methyl alcohol [□: isomerization of **2f**; ○ and ●: isomerization of **2g** (○: set c → set d in Figure 8; ● set a → set b in Figure 8)].

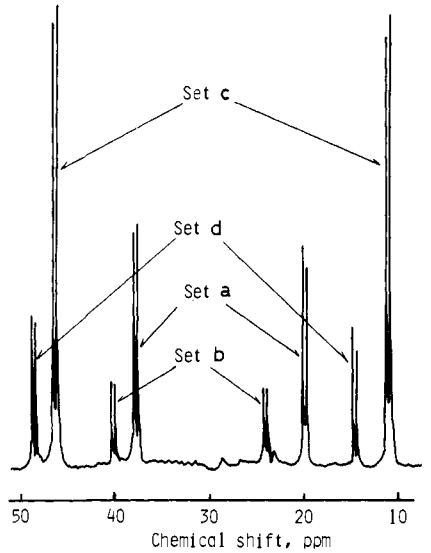

Figure 8. $^{31}P\{^1H\}$ NMR spectrum taken after addition of *trans*-renorphos to **1b** in methyl alcohol at 10 °C.

the following grounds. (1) The four sets of two doublets are classified into two categories, one having large chemical shift differences between each paired doublets (Δ = ca. 40 ppm in Table II) and another with small chemical shift diferences (Δ = ca. 5 ppm). Since *S*- and *R*-configurations of **2c** and **2d** do not greatly affect the chemical shift differences, the large difference between the values is attributed to the difference in the trans and cis geometry of the complexes. (2) *R*-prophos reportedly takes λ conformation on coordination to transition metal.[21,22] In the λ conformation, the phenyl groups of (*R*)-prophos are considered to take an edge-face arrangement opposite to that shown in Figure 5. Oliver and Riley,[27] reported that the edge-face arrangement concerning two Ph rings at P^1 of (*R*)-cycphos was rigid whereas

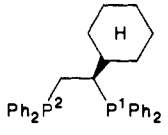

(*R*)-cycphos

the edge-face relation of the other two Ph rings at P^2 was flexible and might be free to rotate in solutions. If the same situation holds for the present (*R*)-prophos-coordinated complexes, de attained with the cis type complex of **2e** is considered to be higher than de attained with the trans type complex, because the Cα configuration will be more strongly affected by the more rigid arrangement of the edge-face phenyl groups situated at closer positions to the Cα carbon. Thus (***R*)-*cis*-2e** is expected to be the predominant species in the equilibriated cis type complexes. The de value and the predominant species in the cis type **2e** complex (Table III) agree with the assumption.

In the case of the (*R*)-prophos complex, the $^{31}P\{^1H\}$ NMR spectrum shows only a small change in the de value with time, suggesting that the *R* to *S* or *S* to *R* isomerization is very fast with the complex to attain the equilibration very rapidly.

***trans*-Cypenphos.** Addition of *trans*-cypenphos to **1b** leads to the formation of two sets of diastereomers, diastereomer-α's and diastereomer-β's, each set consisting of two enantiomers. The $^{31}P\{^1H\}$ NMR spectrum shows two sets of two doublets, similarly to the $^{31}P\{^1H\}$ NMR spectrum of **2c** and **2d**.

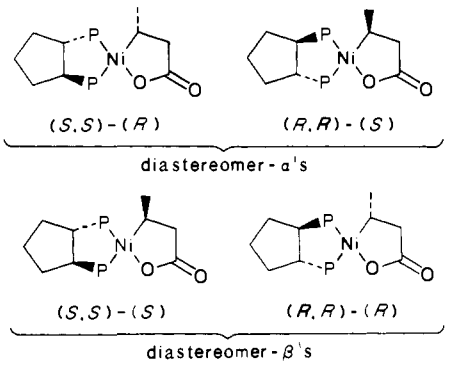

If we assume that (*S*,*S*)-*trans*-cypenphos prefers δ conformation and thus induce (*S*)-asymmetry at the nickel-containing cyclic ester ring in the equilibrated reaction mixture, the NMR peaks are assigned as shown in Table II. Change of the $^{31}P\{^1H\}$ NMR spectrum with time reveals that the initially formed reaction mixture contains a thermodynamically less stable species (presumably diastereomer-α's) as the predominant species, and they are isomerized to their more stable isomers obeying first-order kinetics (**2f**, Figure 7 and Table III).

***trans*-Renorphos.** The $^{31}P\{^1H\}$ NMR spectrum taken after addition of *trans*-renorphos to **1b** shows four sets (set a–set d) of two doublets (Figure 8), corresponding to the following four sets of diastereomers. As shown in Figure 8, the chemical shift

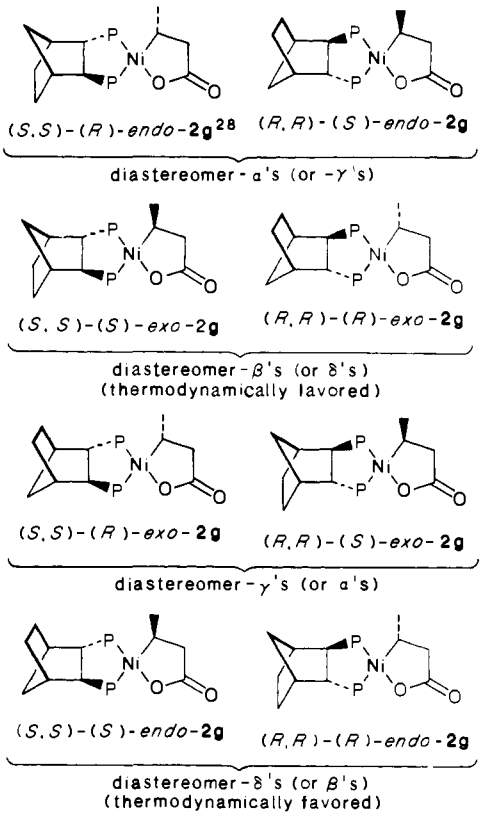

(27) Oliver, J. D.; Riley, D. P. *Organometallics* **1983**, *2*, 1032–1038.

differences between the pairs of doublets (Δ in Table II) are small for sets a and b, whereas they are large for sets c and d.

The $^{31}P\{^1H\}$ NMR spectrum of the renorphos complexes changes with time. The intensities of the signals of set b and set d increase with time with decreases in intensities of signals of set a and set c, respectively. The spectral change reveals again that kinetically favored diastereomers are isomerized to the thermodynamically favored diasteromers. The isomerization roughly obeys the first-order kinetics (Figure 7), and the first-order rate constants are given in Table III.

For assignment of set a–set d we assume again that (i) the chirality in the nickel-containing cyclic ester ring does not affect much the chemical shift difference as in the case of (*R*)-prophos and (ii) that (*S*,*S*)-*trans*-renorphos induces (*S*)-asymmetry at the equilibrated nickel-containing cyclic ester.

On the basis of the assumption the set a and set b are assigned to diastereomer-α's (or γ's) and diastereomer-β's (or δ's), respectively, and the set c and set d are assigned to diasteromer-γ's (or α's) and diastereomer-δ's (or β's).

The high de value (84 and 74%, Table III) observed for the equilibrated mixtures of **2g** may be related to the very rigid structure of *trans*-renorphos.

Conclusion

(i) Coordination of diphosphine to the six-membered nickel complex $NiCH_2CH_2CH_2COO$ with *n*-alkyl group causes a ring contraction reaction affording (diphosphine)$NiCH(CH_3)CH_2COO$, **2**, with *sec*-alkyl group. Employment of chiral diphosphines induces asymmetry in **2**. (ii) As for **2** coordinated by (*S*,*S*)-chiraphos, and (*R*)-prophos, the *R* or *S* configuration at the α-carbon of $NiCH(CH_3)CH_2COO$ in kinetically obtained mixtures coincides with the configuration of α-carbon of amino acids obtained by hydrogenation of olefins catalyzed by rhodium complexes coordinated with the chiral diphosphines. However, the kinetically induced asymmetry at the α-carbon of $NiCH(CH_3)CH_2COO$ is opposite to the thermodynamically induced asymmetry. (iii) Isomerization from the kinetically produced chiral complex to the thermodynamically more stable complex of opposite chirality obeys the first-order kinetics. (iv) The kinetic and thermodynamic asymmetry induction has been elucidated by considering the effect of edge-face array of the aryl rings of the chiral diphosphines around nickel.

Experimental Section

Materials. (*S*,*S*)-chiraphos and (*R*)-prophos were purchased from Strem Chemicals Inc. As for (*R*,*R*)-dipamp, *trans*-cypenphos, *trans*-renorphos, and (*R*)-3-methylsuccinic anhydride, see Acknowledgment. Complex **1a** and **1b** were prepared according to literature.[11-13] $Ph_2PCD_2CD_2PPh_2$ (dpe-d_4) was prepared as reported.[10] Commercially available $Ni(cod)_2$ was recrystallized from hot toluene. Solvents were dried, distilled under N_2 or Ar, and stored under N_2 or Ar. 4-Methylglutaric anhydride was prepared according to literature.[29]

Analysis and Spectroscopic Measurement. Microanalysis of C and H was performed by T. Saito of our laboratory with Yanagimoto CHN Autocorder MT-2. GLC analysis of organic products was performed with Shimadzu GC-3BT gas chromatograph. IR spectra were recorded on a Hitachi Model 295 spectrometer, ^1H NMR spectra on a JEOL Model JNM-PS-100 spectrometer, and ^{13}C- and ^{31}P NMR spectra on JEOL Model JNM-PFT-PS-100 Fourier transform spectrometer.

Ring Contraction. The ring contraction reaction of **1b** to **2a** by addition of dpe was carried out as reported in our previous paper.[12] Dissolution of **1a** in CD_2Cl_2 or methyl alcohol in a temperature range of −78 °C to room temperature caused instant ring contraction as demonstrated by $^{31}P\{^1H\}$ NMR spectrum. The reaction of **2a** with CO (1 atm) in CH_2Cl_2 for 1 h at room temperature afforded 1 mol of 3-methylsuccinic anhydride per 1 mol of **2a**. The reaction of a dispersion of solid **1a** in hexane with CO (1 atm) for 48 h at room temperature afforded 0.41 mol of glutaric anhydride and 0.08 mol of 3-methylsuccinic anhydride per 1 mol of **1a**. The data in Table I were obtained as follows: a mixture of $Ni(cod)_2$, glutaric anhydride (1 mol/1 mol of $Ni(cod)_2$), and ligand was stirred in THF at temperature shown in Table I. After the prescribed reaction time, the amount of intact glutaric anhydride was determined by GLC. All the reaction systems obtained by adding the ligands listed in Table I were homogeneous. Carbon monoxide (1 atm) was then added to the reaction system, and after treating the reaction system with CO for 30 min at room temperature, the amounts of glutaric anhydride and 3-methylsuccinic anhydride were determined by GLC. The amount of glutaric anhydride formed by the reaction of complex **2** and CO was calculated as described in footnote e of Table I.

Acknowledgment. We express our grateful acknowledgement to Dr. Knowles of Monsanto Co. for donating (*R*,*R*)-dipamp through Professor Ojima of State University of New York. We gratefully acknowledge Professor Consiglio of Swiss Federal Institute of Technology for donating *trans*-cypenpho and *trans*-renorphos. Thanks are due to Dr. Ikariya of Tokyo University for donating (*R*)-3-methylsuccinic anhydride. This work was supported by a Grant-in-Aid for Special Project Research from the Ministry of Education, Science and Culture, Japan.

Registry No. 1a, 82840-52-6; **1c**, 105727-73-9; **1d**, 105727-74-0; **1e**, 105727-75-1; **1f**, 105727-80-8; **1g**, 105727-81-9; **2a**, 82840-54-8; (*R*)-**2c**, 91871-18-0; (*S*)-**2c**, 91926-62-4; (*R*)-**2d**, 105727-76-2; (*S*)-**2d**, 105814-81-1; (*R*)-*cis*-**2e**, 105727-77-3; (*R*)-*trans*-**2e**, 105814-82-2; (*S*)-*cis*-**2e**, 105814-83-3; (*S*)-*trans*-**2e**, 105814-84-4; (*S*,*S*)-(*R*)-**2f**, 105814-91-3; (*R*,*R*)-(*S*)-**2f**, 105816-40-8; (*S*,*S*)-(*S*)-**2f**, 105814-92-4; (*R*,*R*)-(*R*)-**2f**, 105727-82-0; (*S*,*S*)-(*R*)-*endo*-**2g**, 105727-78-4; (*R*,*R*)-(*S*)-*endo*-**2g**, 105814-86-6; (*S*,*S*)-(*S*)-*exo*-**2g**, 105814-90-2; (*R*,*R*)-(*R*)-*exo*-**2g**, 105814-87-7; (*S*,*S*)-(*R*)-*exo*-**2g**, 105814-88-8; (*R*,*R*)-(*S*)-*exo*-**2g**, 105814-89-9; (*S*,*S*)-(*S*)-*endo*-**2g**, 105814-85-5; (*R*,*R*)-(*R*)-*endo*-**2g**, 105816-39-5; **6c**, 91871-17-9; **6d**, 105727-83-1; **6e**, 105727-79-5; dmpe, 23936-60-9; bpy, 366-18-7; (*S*,*S*)-chiraphos, 64896-28-2; (*R*,*R*)-diamp, 55739-58-7; (*R*)-prophos, 67884-32-6; PMe_2Ph, 672-66-2; PEt_3, 554-70-1; PBu_3, 998-40-3; $PMePh_2$, 1486-28-8; PEt_2Ph, 1605-53-4; $PEtPh_2$, 607-01-2; PPh_3, 603-35-0; $Ni(cod)_2$, 1295-35-8; 3-methylsuccinic anhydride, 4100-80-5; gluturic anhydride, 108-55-4.

(28) Notation to describe steric relation between the α-CH_3 in the nickel-containing cyclic ester ring and *trans*-renorphos.

(29) Calson, J. *Organic Syntheses*; Wiley: New York, 1963; Collect. Vol. 4, pp 630–633.